Eur. Phys. J. A (2016) **52**: 166
DOI 10.1140/epja/i2016-16166-2

THE EUROPEAN PHYSICAL JOURNAL A

Regular Article – Experimental Physics

Search for two-phonon octupole excitations in ^{146}Gd

J.N. Orce[1,a], M. Kumar Raju[1,2], N.A. Khumalo[1,2,3], T.S. Dinoko[1,2], P. Jones[2], R.A. Bark[2], E.A. Lawrie[2], S.N.T. Majola[2,4], L.M. Robledo[5], B. Rubio[6], M. Wiedeking[2], J. Easton[1,2], E.A. Khaleel[2,7], B.V. Kheswa[2,7], N. Kheswa[2,1], M.S. Herbert[1], J.J. Lawrie[2], P.L. Masiteng[1,2,b], M.R. Nchodu[2], J. Ndayishimye[2,7], D. Negi[2], S.P. Noncolela[1,2], S.S. Ntshangase[3], P. Papka[2,7], D.G. Roux[8], O. Shirinda[1,2], P.S. Sithole[1,2], and S.W. Yates[9]

[1] Department of Physics, University of the Western Cape, P/B X17, Bellville 7535, South Africa
[2] iThemba LABS, P.O. Box 722, Somerset West 7129, South Africa
[3] Department of Physics and Engineering, University of Zululand, KwaDlangezwa, 3886, South Africa
[4] Department of Physics, University of Cape Town, Private Bag, 7701 Rondebosch, South Africa
[5] Departamento de Física Teórica, Universidad Autónoma de Madrid, E-28049 Madrid, Spain
[6] Instituto de Física Corpuscular, CSIC-Universidad de Valencia, E-46071 Valencia, Spain
[7] Department of Physics, University of Stellenbosch, Private Bag X1, 7602 Matieland, South Africa
[8] Department of Physics and Electronics, Rhodes University, Grahamstown 6410, South Africa
[9] Departments of Chemistry and Physics + Astronomy, University of Kentucky, Lexington, KY 40506-0055, USA

Received: 20 March 2016 / Revised: 24 May 2016
Published online: 24 June 2016 – © Società Italiana di Fisica / Springer-Verlag 2016
Communicated by D. Pierroutsakou

Abstract. The low-spin structure of the nearly spherical nucleus ^{146}Gd was studied using the ^{144}Sm(^{4}He, 2n) fusion-evaporation reaction. High-statistics γ-γ coincidence measurements were performed at iThemba LABS with 7×10^{9} γ-γ coincidence events recorded. Gated γ-ray energy spectra show evidence for the $6_2^+ \rightarrow 3_1^- \rightarrow 0_1^+$ cascade of $E3$ transitions in agreement with recent findings by Caballero and co-workers, but with a smaller branching ratio of $I_\gamma = 4.7(10)$ for the $6_2^+ \rightarrow 3_1^-$ 1905.1 keV γ ray. Although these findings may support octupole vibrations in spherical nuclei, sophisticated beyond mean-field calculations including angular-momentum projection are required to interpret in an appropriate way the available data due to the failure of the rotational model assumptions in this nucleus.

1 Motivation

According to Bohr and Mottelson's description of surface vibrations, the lowest-lying collective excitations in nuclei near closed shells arise from quadrupole and octupole surface vibrations; $\lambda = 2$ and $\lambda = 3$, respectively, in the multipole expansion of the nuclear surface [1]. However, the breakdown of $\lambda = 2$ multi-phonon structures in the Cd isotopes (see ref. [2] and references therein) demands a re-examination of low-excitation surface vibrations. This work aims at the exploration of two-phonon octupole vibrations in the nearly spherical nucleus $^{146}_{64}$Gd$_{82}$.

The simple harmonic oscillator predicts a two-phonon $3^-\otimes3^-$ quartet ($J^\pi = 0^+$, 2^+, 4^+ and 6^+) of states at approximately twice the excitation energy of the first 3_1^- octupole phonon state to decay with $B(E3)$ transition probabilities about twice that of the $3_1^- \rightarrow 0_1^+$ transition [3,1]. Anharmonicities may arise from particle-phonon couplings and the effect of the Pauli principle between the particle-hole components of the phonons [4–6]. Although many examples of low-lying 3_1^- excitations which decay with large $E3$ strengths are known [7], observation of multi-phonon excitations of the octupole type are scarce.

A firm candidate for a two-phonon octupole excitation built on the ground state of ^{208}Pb has been observed [8, 9] as a cascade of two $E3$ transitions from a 0^+ state at 5241 keV ($0^+ \rightarrow 3^- \rightarrow 0^+$). More complicated two-phonon octupole excitations built on single-particle excitations have also been identified in nuclei near $N = 82$ [4–6,10]. In ^{147}Gd, the two-phonon octupole mode was first characterized from a cascade of two enhanced $E3$ transitions associated with the stretch-coupled $(\nu f_{7/2}\otimes3^-\otimes3^-)19/2^-$ configuration [4]. Additional cascades of $E3$ transitions have been identified in the neighbouring $N = 84$ isotones ^{144}Nd [10], ^{146}Sm [10], and ^{148}Gd [5,6], but only in the latter case are the states fully characterized with $E3$ transition rates. In each of these nuclei, the identifications by the characteristic $E3$-$E3$ cascades were possible because the two-phonon states are fortuitously yrast. Because these states involve the coupling of particles to the two-phonon

[a] e-mail: jnorce@uwc.ac.za
[b] *Present address:* University of Johannesburg, Department of Physics, P.O. Box 524, Auckland Park 2006, South Africa.

octupole excitation (*e.g.*, $\nu^2 \otimes 3^- \otimes 3^-$ in ^{148}Gd) their descriptions are complex.

The nucleus ^{146}Gd is the only known even-even nucleus besides ^{208}Pb with a 3^- first-excited state, thus two-phonon octupole excitations have long been sought. However, only recently, based on experimental evidence from the ^{144}Sm(^{4}He, 2n) reaction, has the 3484.1 keV 6_2^+ state in ^{146}Gd been identified as the highest-spin member of the $3^- \otimes 3^-$ quartet by Caballero and co-workers [11]. A 1905.8(6) keV γ ray, representing a small branch from the 3484.1 keV level, is observed to feed the 3_1^- state at 1579.4 keV, and is the first observation of a $6^+ \rightarrow 3^- \rightarrow 0^+$ $E3$ cascade in an even-even nucleus. Angular distribution and γ-ray linear polarization data firmly supported the $J^\pi = 6^+$ assignment [11]. Additional candidates for these two-phonon octupole states were also suggested [11]; however, a complete characterization of the crucial 1905.8 keV γ ray is still desirable [11].

2 Experimental details

Yrast and non-yrast states in ^{146}Gd have been populated at the iThemba Laboratory for Accelerator Based Sciences (iThemba LABS) using the ^{144}Sm(^{4}He, 2n$\gamma\gamma$)^{146}Gd fusion-evaporation reaction at beam energies ranging from $E_{lab} = 26.1$ to 26.8 MeV, with an energy spread of about 0.2 MeV. An optimum beam energy of about 26.3 MeV was chosen from excitation-function measurements by Yates and co-workers [12] to enhance the population of non-yrast states in ^{146}Gd. The ^{4}He$^+$ ions were delivered by the $K = 200$ Separated Sector Cyclotron with beam pulses separated by 60 ns and bombarded a self-supporting 3 mg/cm^2 ^{144}Sm target enriched to 85.9%, with small contributions from the heavier Sm isotopes. Time correlated γ-ray events were collected using the AFRODITE array [13] comprising eight escape-suppressed clover detectors, four positioned at 90° and four at 135° with respect to the beam axis. Each clover detector consists of four n-type coaxial HPGe crystals with dimensions of 70 mm length and 50 mm front diameter. The crystals are placed 19.6 cm from the target centre position in the AFRODITE standard configuration for γ-γ coincidence measurements.

A γ-γ trigger with a prompt time window of $\Delta t = 150$ ns between two γ rays being detected by two separate clovers in the AFRODITE array characterized the γ-γ coincidence events. Beam currents from 15 to 50 pnA were used and a total of about 9.5×10^9 γ-γ coincidence events were accumulated after add-back corrections during nine days of beam time. Four γ-γ coincidence experiments were performed using the ^{144}Sm(^{4}He, 2n) reaction: 1) two consecutive weekends in November-December 2011 ($E_{lab} = 26.3$ and 26.8 MeV, respectively) using an analog electronics system, and 2) two weekends in early July and late August 2012 with a XIA digital electronics system ($E_{lab} = 26.1$ and 26.7 MeV, respectively). Prior to these experiments, the digital parameters were optimised for detector resolution. Higher statistics were collected with the digital system at the end of the experiment reaching a maximum of 40 kHz coincidence rate and 60 kHz singles count rate (per clover). Comparatively, only about 6 and 13 kHz coincidence rates and 15 and 30 kHz singles rates were collected on average during the previous runs using the analog and digital systems, respectively. For each experiment, decay data from ^{56}Co and ^{152}Eu radioactive sources were taken for energy and efficiency calibrations.

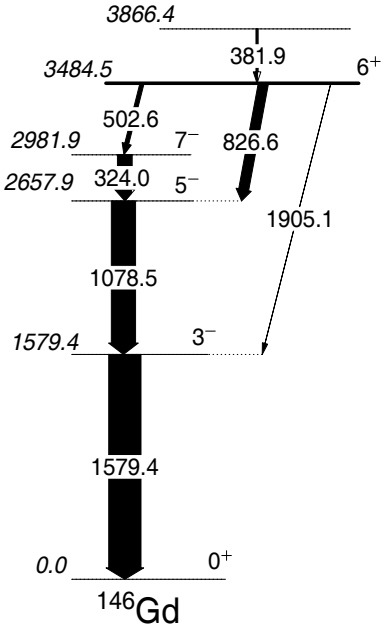

Fig. 1. Partial level scheme of ^{146}Gd based on the 381.9 and 1579.4 keV gated γ-ray spectra. The thicknesses of the arrows are proportional to the competing branches (relative intensities).

3 Data analysis and discussion

In the offline analysis, γ-γ coincident events were unfolded from the raw data and replayed into RADWARE format [14] for subsequent analysis. Relevant contaminants in this work included ^{147}Gd from the ^{144}Sm(^{4}He, n) reaction, ^{144}Sm from Coulomb excitation, and ^{156}Gd from the ^{154}Sm(^{4}He, 2n) reaction (2.1% of ^{154}Sm was present in the target). The total projections indicate a larger background arising from random γ-γ coincidences in the digital system. In order to minimize the effects of randoms, time windows of $\Delta t = 100$, 150 and 200 ns were set to construct different coincidence matrices offline. A shorter time coincidence window of 100 ns presented considerably fewer randoms and a better peak-to-background ratio for gated spectra. Therefore, $\Delta t = 100$ ns was applied to all the matrices constructed in this work with a corresponding reduction of the total coincidence events to 7×10^9. In addition, a delayed matrix which included random events with another 100 ns time window was subtracted from the prompt matrix. Summing effects were investigated and found to be negligible with the standard configuration of the AFRODITE array. The partial level scheme confirmed by this work is shown in fig. 1.

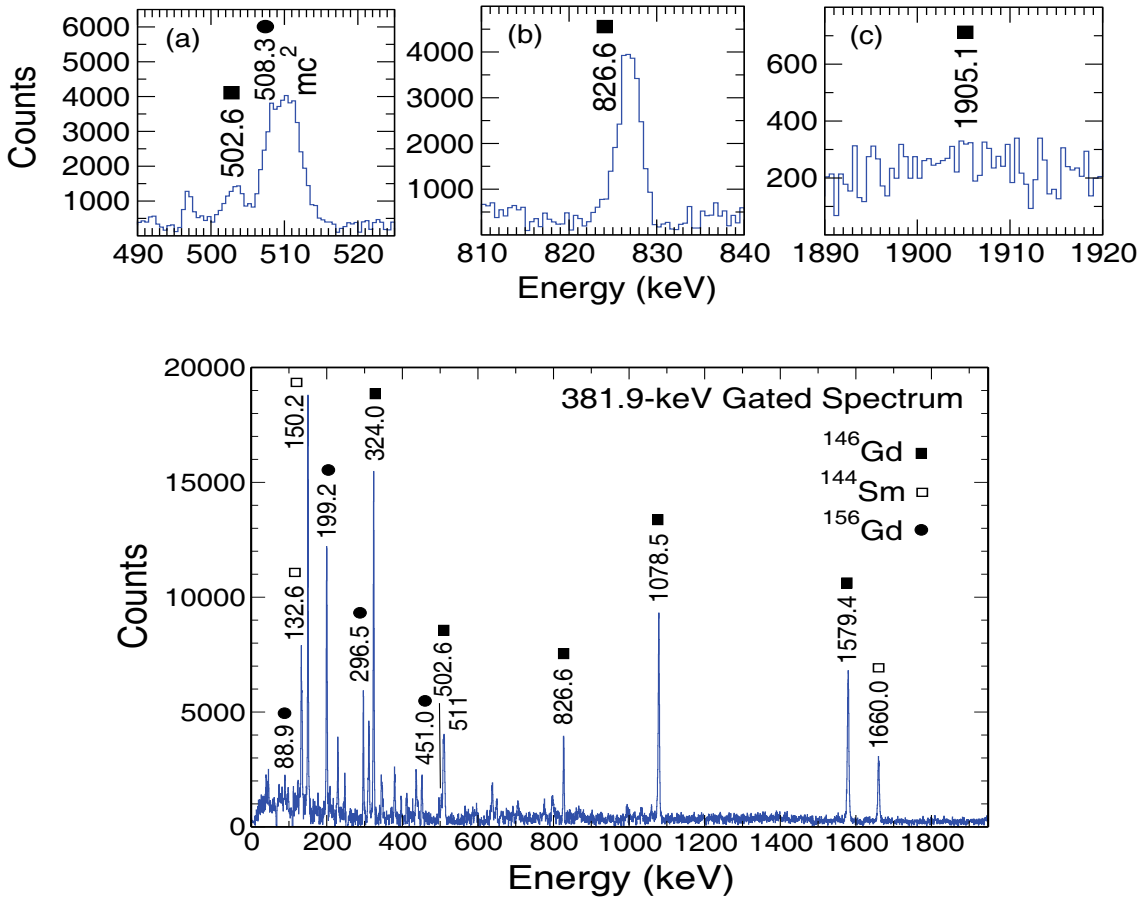

Fig. 2. Gamma-ray spectrum gated on the 381.9 keV γ ray. The top panels are expansions of regions of interest.

Figure 2 shows a background-subtracted γ-ray spectrum gated on the 381.9 keV γ ray, as deduced from the total (analog+digital) data. Besides γ rays from ^{146}Gd, there are additional γ rays de-exciting Coulomb-excited states up to 2.324 MeV in ^{144}Sm and, because of isotopic impurities in the target, transitions from the ground-state band in ^{156}Gd. In ^{144}Sm, there is a 380.7 keV γ ray in coincidence with the 150.2, 132.6 and 1660.0 keV γ rays [15]. More problematic, regarding the background around the 502.6 keV peak depopulating the 6_2^+ state of interest in ^{146}Gd, is the 380.4 keV γ ray in ^{156}Gd which is in coincidence with the 508.3 keV transition. Figure 2 shows the 502.6 keV and 826.6 keV γ rays (fig. 2(a) and fig. 2(b), respectively) depopulating, as shown in the decay scheme in fig. 1, the 3484.5 keV level of interest in ^{146}Gd, in agreement with the previous work [11]. The 1905.8 keV γ ray is not clearly observed in fig. 2(c). Slightly lower statisitics but a superior peak-to-background ratio were achieved in the 381.7 keV gated spectrum of Caballero *et al.* [11,16]. Note that the γ rays of interest in this work were assigned energies of 381.7(3), 502.6(1), 826.7(1), and 1905.8(6) keV in ref. [11].

The multipolarity of the 826.6 keV transition can be studied with the directional correlation from oriented states (DCO) method [17]. The experimental DCO ratio, R_{DCO}, can be defined as

$$R_{DCO} = \frac{I(\gamma_1(\theta_1), \gamma_2(\theta_2))}{I(\gamma_1(\theta_2), \gamma_2(\theta_1))}, \tag{1}$$

where $\theta_1 = 90°$, $\theta_2 = 135°$, and γ_1 is the transition whose multipolarity is to be determined when gating on the stretched $E2$ γ_2 transition. R_{DCO} values of ≈ 0.6 and ≈ 1.0 are generally found for stretched dipole and stretched $E2$ transitions, respectively [18]. A value of $R_{DCO} = 0.71(7)$ is determined for the 826.6 keV γ ray by gating on the 1078.5 keV stretched $E2$ transition, which confirms the stretched dipole character of the 826.6 keV transition.

Furthermore, the linear polarization sensitivity of the ring of clover detectors at $\theta \approx 90°$ [19] was utilised to determine the character of the 826.6 keV dipole transition depopulating the 3484.5 keV level. A higher polarization sensitivity is obtained by requiring the add-back events to obey the Compton formula for photon scattering through angles $\theta \approx 90°$ [20]. The linear polarization asymmetry A_p is given by

$$A_p = \frac{a(E_\gamma)N_\perp - N_\parallel}{a(E_\gamma)N_\perp + N_\parallel}; \tag{2}$$

Table 1. Normalized relative intensities, I_γ, measured in this and previous work [16] for the γ rays depopulating the 6^+ state at 3484.5 keV in ^{146}Gd.

E_γ (keV)	I_γ (current work)		I_γ [16]
	381.9 keV gate	1579.4 keV gate	381.7 keV gate
826.6(1)	100(6)	100(4)	100(7)
502.6(1)	20(2)	21(1)	16(2)
1905.1(3)	< 4.3	4.7(10)	6(3)

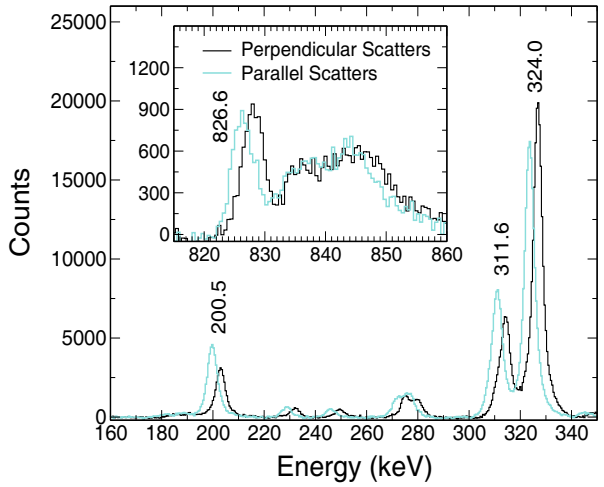

Fig. 3. Linear polarization spectra shifted by 2 keV showing the distinction between perpendicular and parallel components for known magnetic (200.5 keV, 311.6 keV) and electric (324.0 keV) transitions and the 826.6 keV transition shown in the inset.

where $N_\parallel$ and $N_\perp$ are the number of Compton-scattered γ rays in the planes parallel and perpendicular to the reaction plane, respectively. The asymmetry correction factor $a(E_\gamma) = \frac{N_\parallel}{N_\perp}$ at different γ-ray energies has been extracted from non-polarized γ rays from a ^{152}Eu source yielding $a(E_\gamma) = 1.01(2)$.

Figure 3 shows polarization spectra gated on the 1078.5 + 1579.4 keV γ rays. The normalized parallel, $N_\parallel$, and perpendicular, $a(E_\gamma)N_\perp$, scattered events are represented by cyan and black colors, respectively. The deduced magnetic nature of the 311.6 keV transition based on $A_p = -0.09(2)$ and the measured electric nature of the 324.0 and 1078.5 keV stretched quadrupole transitions based on $A_p = +0.06(1)$ and $+0.04(1)$, respectively, are in agreement with recent work done by Krishichayan and collaborators using a heavy-ion reaction and the same type of clover detector [21]. For the 826.6 keV γ ray, the inset spectrum shows that the perpendicular-scattered events are slightly larger, yielding a polarization ratio of $+0.05(2)$, hence, in agreement with the $E1$ character and supporting the $J^\pi = 6^+$ assignment.

Branching ratios for the 502.6 and the 826.6 keV γ rays and a upper limit on the 1905.1 keV relative intensity, I_γ, have been determined from the 381.9 keV gated spectrum in fig. 2 and are listed in table 1. The relative intensity for each γ ray has been measured considering the γ-ray efficiencies. The branching ratios are, within limits, in agreement with previous work [16]. An upper limit for the 1905.1 keV peak area has been determined using Currie's procedure [22,23], which assumes that the background counts in the spectrum follow a normal Gaussian distribution. The upper limit for the peak area, A, is given by

$$A = 1.746 \text{ FWHM } \sigma_b, \tag{3}$$

where FWHM is the full width at half maximum of the Gaussian and σ_b is the background standard deviation, where $\sigma_b = \sqrt{\frac{1}{N}\sum_i (x_i - \bar{x})^2}$, with N the number of channels in the distribution, x_i the number of counts per channel and $\bar{x}$ the mean value. As listed in table 1, the resulting upper limit for the normalized relative intensity is 4.3, which is in agreement with the lower limit, $I_\gamma = 6(3)$, measured in previous work [16].

An additional γ-ray spectrum gated on the 1579.4 keV γ ray is shown in fig. 4. Branching ratios for the 502.6, 826.6 and 1905.1 keV γ rays have been determined from this spectrum and are listed in table 1. In this particular case the relative intensities could be extracted directly since there is no branching in the de-excitation of the 2981.9 and 2657.9 keV levels. The broader peak centered at around 1902 keV in the top panel of fig. 4 is a triplet feature of previously observed 1898.0, 1901.5 and 1905.1 keV peaks [16]. A fit to the data provides three distinct γ-ray peaks corresponding to these energies. The fit considered a fixed FWHM = 4 keV, as this was approximately the FWHM found for other single γ-ray peaks in this region. No other energy gates show evidence for the 1905.1 keV γ ray. The fit to the 1905.1 keV peak shown in the top panel of fig. 4 yields $I_\gamma = 4.7(10)$, which is consistent with the upper limit determined from the 381.9 keV gated spectrum and in agreement with the previous work [11].

Octupole properties of many even-even nuclei were obtained [24] with the Generator Coordinate Method (GCM) using the axial octupole moment Q_{30} as generating coordinate. In this calculation the excitation energy of the lowest octupole state as well as the $B(E3)$ strength to the ground state were obtained for the three parametrizations of the Gogny force, namely D1S, D1M and D1N. Systematic deviations were identified in spherical nuclei with too large excitation energies and too small transition strengths. An explanation for the first is still under debate but the reason for the small transition strengths was traced back [25] to the breaking down of the rota-

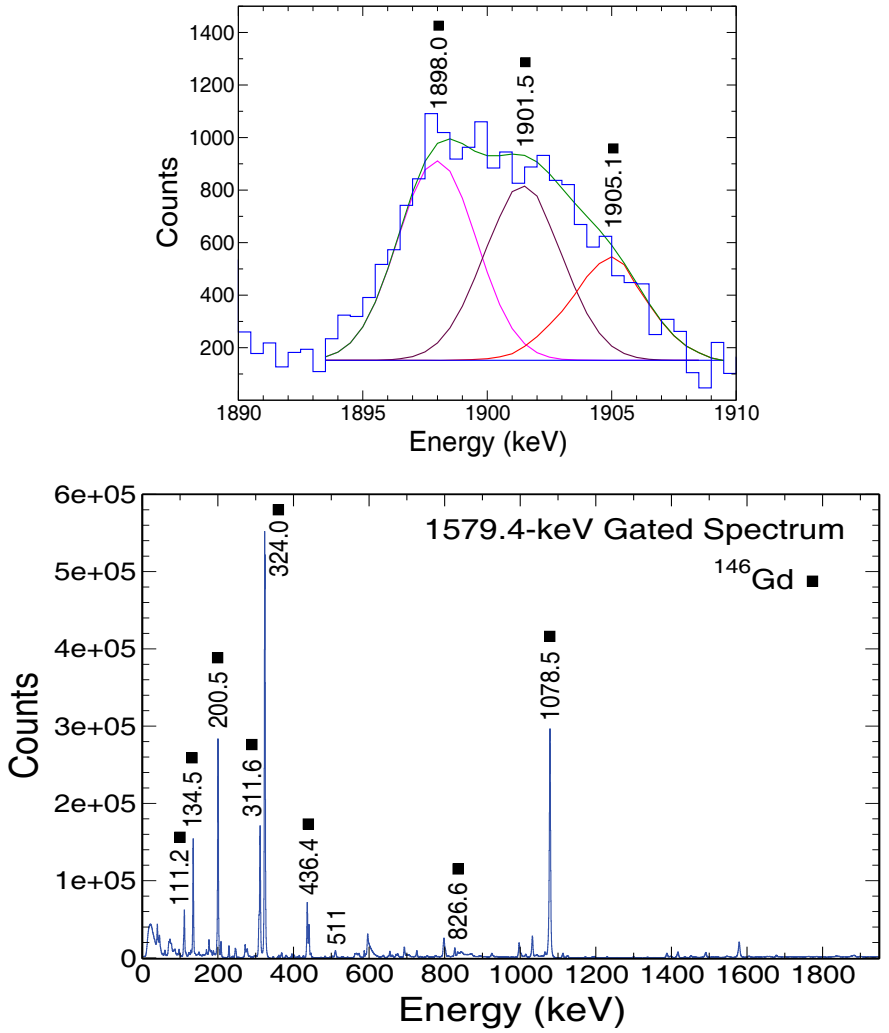

Fig. 4. Gamma-ray spectrum gated on the 1579.4 keV γ ray. The top panel expands the region of interest and shows the fit to the 1905.1 keV peak.

Table 2. Theoretical results obtained with GCM calculations for one- and two-phonon excitations (1p and 2p, respectively) using the Gogny D1S force. Energies are given in MeV and $B(E3)$ strengths in Weiskopft units (1 W.u. = 0.0594 $A^2\,e^2\,fm^6$).

Calculation	E_{1p}	E_{2p}	$B(E3, 3^-_{1p} \to 0^+)_{(ROT)}$	$B(E3, 3^-_{1p} \to 0^+)_{(PROJ)}$	$B(E3, 0^+_{2p} \to 3^-)_{(PROJ)}$	$B(E3, 6^+_{2p} \to 3^-)_{(PROJ)}$
GCM-Q_3	3.19	6.40	9.57	24.44	4.35	54.07
GCM-Q_2-Q_3	3.23	7.09	9.53	–	–	–

tional formula in soft nuclei. In those cases, the use of full-fledged angular-momentum–projected wave functions is required. In this GCM calculations a harmonic-oscillator pattern emerges when the ground state is reflection symmetric and the energy as a function of the octupole moment resembles a parabola. The first (negative parity) excited state resembles an one-phonon octupole whereas the second (positive parity) corresponds to a two-phonon octupole state. Other alternative descriptions of two-phonon octupole excitations are mostly based on extensions of the Interacting Boson Model (IBM) to include negative-parity bosons [26–30], see also [31] for a review including additional methods.

Here we report on a GCM calculation with Gogny D1S for ^{146}Gd, where not only the first excited state is considered but also the 0^+, 2^+, 4^+ and 6^+ states corresponding to the two-phonon octupole excitations. The $E3$ transitions strengths are computed both using the traditional rotational formula (which is hardly justified in this spherical nucleus but is given here as a reference) as well as the full-fledged method using angular-momentum–projected wave functions. The results obtained with Gogny D1S in the GCM-Q_3 calculation are summarized in the first row of table 2. Too high excitation energies are obtained for the 3^- state (3.19 MeV) and the two-phonon octupole states located at twice the excitation energy. The

$B(E3; 3^-_{1p} \rightarrow 0^+)$ value of 9.57 W.u. computed with the rotational formula (ROT) falls too short as expected for this nearly spherical state. However, the projected calculation (PROJ) gives a much higher value of 24.44 W.u. The failure of the rotational formula is a direct consequence of the sphericity of the ground state of ^{146}Gd. Similar enhancements of $B(E3)$ transitions, as compared to the rotational formula, have been observed, for instance, in ^{208}Pb [32]. The $B(E3)$ transition from the 0^+ built on the two-phonon octupole to the 3^- is 4.35 W.u. (see table caption for the definition of a W.u.) which is severely quenched with respect to the rotational formula prediction. On the other hand, the calculation of the $B(E3)$ transition from the observed 6^+ built on the two-phonon octupole state to the 3^- yields 54.07 W.u. These results have to be compared with the ones quoted in [11] and obtained with a two-phonon octupole model: $B(E3; 3^-_{1p} \rightarrow 0^+) = 37$ W.u. and $B(E3; 6^+_{2p} \rightarrow 3^-) = 56$ W.u. The results of [11] are consistent with our projected results.

A side product of the angular-momentum–projected calculation is that we can obtain the probability amplitude of each angular momentum J in the different intrinsic configurations considered. In the ground state the $J = 0$ wave function probability is 87%. For the one-phonon octupole is the $J = 3^-$ state which has the largest probability amplitude: 74%. Finally, for the two-phonon octupole intrinsic states the probability distribution is more evenly distributed but the $J = 6^+$ amplitude is the largest with a 25% of probability. These numbers give us confidence on the assignment made to the intrinsic states obtained in the GCM.

The coupling with the quadrupole degree of freedom has been taken into account in a GCM calculation using the collective variables Q_{20} and Q_{30} as generating coordinates (see refs. [33,34] for similar calculations in the rare earths and the actinides). The results listed in the second row of table 2 indicate that both degrees of freedom are essentially uncoupled. The coupling between Q_{20} and Q_{30} slightly pushes up the energy of the two-phonon octupole state. Unfortunately, in this case the projected calculation is too demanding for our present computing capabilities. However, it can be argued that given the decoupling between the quadrupole and octupole degrees of freedom, the projected transition strenghts should not differ too much from the GCM-Q_3 results. Work to extend the angular-momentum–projected calculation of transition strengths to the Q_{20} and Q_{30} case are in progress as they will allow the estimation of the $6^+ \rightarrow 5^-$ transition to the 5^- interpreted as a quadrupole-octupole phonon.

4 Conclusions

Summarizing, high-statistics γ-γ coincidence mesurements have been carried out with the ^{144}Sm(^{4}He, 2n) reaction in order to study two-phonon octupole excitations in ^{146}Gd. Angular distribution and γ-ray linear polarization data supported the $J^\pi = 6^+$ assignment for the 3484.5 keV level. Slightly higher statistics for non-yrast states in ^{146}Gd are present in our gated spectra than in previous work [11,16]. The larger background arising from random γ-γ coincidences in the digital system prevented, however, a more sensitive identification of the 1905.1 keV γ ray in our 381.9 keV gated spectrum. The upper limit measured for the relative intensity of the 1905.1 keV γ ray from the 381.9 keV gated spectrum, $I_\gamma < 4.3$, is in agreement with the branching ratio measured from the 1579.4 keV gated spectrum, $I_\gamma = 4.7(10)$, and supports the placement of the 1905.1 keV γ ray. Branching ratios for the 502.6, 826.6 and 1905.1 keV γ rays depopulating the 6^+_2 state at 3.484 MeV are in agreement with recent work by Caballero and co-workers. These findings provide evidence for a cascade of $6^+ \rightarrow 3^- \rightarrow 0^+$ $E3$ γ rays. An analysis of the spectroscopic features of two-phonon vibrations in spherical nuclei using modern mean-field calculations using the axial octupole moment Q_{30} as generating coordinate and the Gogny force predicts a strong $B(E3)$ strength for the $6^+ \rightarrow 3^-$ transition. The fundamental question about the existence of two-phonon octupole vibrations in spherical nuclei remains open. The fact that quadrupole surface vibrations are currently under question [35,36] opens up new theoretical avenues and encourages additional measurements. With the large $6^+ \rightarrow 3^-$ $E3$ strength predicted in this work, the supposedly 6^+ two-phonon state in ^{146}Gd should be easily populated via two-step Coulomb excitation using radioactive ion beams.

This work was supported by the South African National Research Foundation (NRF) under Grant 93500, the Spanish Ministry of Sciences and Technology under Grant under grant FPA2011-24553 and the U.S. National Science Foundation under Grant PHY-1305801. We sincerely thank J.L. Wood for fruitful physics discussions and the accelerator group at iThemba LABS for providing us with excellent beams.

References

1. A. Bohr, B.R. Mottelson, *Nuclear Structure*, Vol. **2** (World Scientific, Singapore, 1998) p. 654.
2. P.E. Garrett, J.L. Wood, J. Phys. G **37**, 064028 (2010).
3. K. Alder *et al.*, Rev. Mod. Phys. **28**, 432 (1956).
4. P. Kleinheinz, J. Styczen, M. Piiparinen, J. Blomqvist, M. Kortelahti, Phys. Rev. Lett. **48**, 1457 (1982).
5. S. Lunardi *et al.*, Phys. Rev. Lett. **53**, 1531 (1984).
6. M. Piiparinen *et al.*, Phys. Rev. Lett. **70**, 150 (1993).
7. T. Kibédi, R.H. Spear, At. Data Nucl. Data Tables **80**, 35 (2002).
8. M. Yeh, P.E. Garrett, C.A. McGrath, S.W. Yates, T. Belgya, Phys. Rev. Lett. **76**, 1208 (1996).
9. M. Yeh *et al.*, Phys. Rev. C **57**, R2085 (1998).
10. L. Bargioni *et al.*, Phys. Rev. C **51**, R1057 (1995).
11. L. Caballero *et al.*, Phys. Rev. C **81**, 031301(R) (2010).
12. S.W. Yates *et al.*, Z. Phys. A **324**, 417 (1986).
13. M. Lipoglavsek *et al.*, Nucl. Instrum. Methods A **557**, 523 (2006).
14. D.C. Radford, Nucl. Instrum. Methods A **361**, 297 (1995).
15. NNDC database, `http://www.nndc.bnl.gov`.
16. L. Caballero, *Double Octupole States in ^{146}Gd*, PhD Thesis, Universidad de Valencia (2005).
17. K.S. Krane *et al.*, Nucl. Data Tables **11**, 351 (1973).

18. C.M. Petrache *et al.*, Phys. Rev. C **74**, 034304 (2006).
19. P.M. Jones *et al.*, Nucl. Instrum. Methods A **362**, 556 (1995).
20. T.S. Dinoko *et al.*, in preparation.
21. Krishichayan *et al.*, arXiv:1308.0119 [nucl-ex].
22. L.A. Currie, Anal. Chem. **40**, 586 (1968).
23. K.L. Green, MSc Thesis, University of Guelph (2009).
24. L.M. Robledo, G.F. Bertsch, Phys. Rev. C **84**, 054302 (2011).
25. L.M. Robledo, G.F. Bertsch, Phys. Rev. C **86**, 054306 (2012).
26. D.F. Kusnezov, E.A. Henry, R.A. Meyer, Phys. Lett. B **228**, 11 (1989).
27. N.V. Zamfir, J.-Y. Zhang, R.F. Casten, Phys. Rev. C **66**, 057303 (2002).
28. N.V. Zamfir, D. Kusnezov, Phys. Rev. C **67**, 014305 (2003).
29. K. Nomura, D. Vretenar, T. Niksic, B.-N. Lu, Phys. Rev. C **89**, 024312 (2014).
30. K. Nomura, R. Rodriguez-Guzman, L.M. Robledo, Phys. Rev. C **92**, 014312 (2014).
31. P.A. Butler, W. Nazarewicz, Rev. Mod. Phys. **68**, 349 (1996).
32. L.M. Robledo, EPJ Web of Conferences **66**, 02091 (2014).
33. R. Rodríguez-Guzmán, L.M. Robledo, P. Sarriguren, Phys. Rev. C **86**, 034336 (2012).
34. L.M. Robledo, P.A. Butler, Phys. Rev. C **88**, 051302 (2013).
35. W.D. Kulp *et al.*, Phys. Rev. C **77**, 061301(R) (2008).
36. P.E. Garrett, J. Phys. G **27**, R1 (2001).